

PREPARATION AND CHARACTERIZATION OF A CipHCl-PLA/PBC/CS COMPOSITE FIBER MEMBRANE FOR ANTIBACTERIAL WOUND DRESSING

PRIPRAVA IN KARAKTERIZACIJA MEMBRANE IZ KOMPOZITNIH VLAKEN NA OSNOVI CipHCl-PLA/PBC/CS ZA ANTIBAKTERIJSKE PREVEZE PO POŠKODBAH

Xiaohua Gu^{1,2*}, Dasheng Zhang¹, Siwen Liu³, Yan Liu⁴

¹College of Innovative Material and Energy, Qiqihar University, Heilongjiang Qiqihar 161006, China

²College of Innovative Material and Energy, Donghua University, Shanghai 201620, China

³College of Innovative Material and Energy, Hubei University, Hubei 430062, China

⁴School of Energy and Building Environment of Guilin University of Aerospace Technology, Guilin, Guangxi 541004, China

Prejem rokopisa – received: 2022-03-08; sprejem za objavo – accepted for publication: 2022-05-09

doi:10.17222/mit.2022.444

In this paper, a polylactic acid (PLA)/polybutylene carbonate (PBC)/chitosan (CS) composite membrane with different mass fractions of ciprofloxacin hydrochloride (CipHCl) drug was prepared through the electrostatic spinning technology. The morphology and chemical structure of the resultant CipHCl-PLA/PBC/CS fiber membranes were characterized with scanning electron microscopy (SEM), Fourier transform infrared spectroscopy (FTIR) and X-ray diffraction (XRD). A drug-release test, bacteriostatic test and cytotoxicity test were performed to determine the drug-release properties, bacteriostatic properties and cytotoxicity, respectively. Results show that the CipHCl-PLA/PBC/CS composite fiber membranes have good biocompatibility. When the CipHCl content is 20 w/%, the average fiber diameter is 374 nm. After 192 h, the drug-release rate of the CipHCl-PLA/PBC/CS composite fiber membrane containing 20 w/% of CipHCl reaches 88.2 %. The antibacterial activity of the CipHCl-PLA/PBC/CS composite fiber membrane is much higher than that of the PLA/PBC composite fiber membrane. Besides, the antibacterial activity of the CipHCl-PLA/PBC/CS composite fiber membrane against *E. coli* is slightly higher than that against *S. aureus*.

Keywords: polylactic acid, polybutylenes carbonate, chitosan, CipHCl, antibacterial activity

V članku avtorji opisujejo pripravo kompozitne membrane na osnovi polilaktične kisline (PLA), polibutilen karbonata (PBC) in hitozana (CS) z različnimi masnimi deleži zdravila na osnovi kiprofloksiacin-hidroklorida (CipHCl). Njeno pripravo so izvedli s tako imenovano tehnologijo elektrostatskega nanosa. Morfologijo in kemijsko strukturo iz kompozitnih vlaken izdelane CipHCl-PLA/PBC/CS membrane so okarakterizirali s pomočjo vrstičnega elektronskega mikroskopa (SEM), Fourierjeve transformacijske infrardeče spektroskopije (FTIR), in rentgenske difrakcije (XRD). Izvedli so preizkuse sproščanja zdravila, bakteriostatične teste in teste citotoksičnosti, da bi določili lastnosti sproščanja učinkovine in bakteriostatičnosti oziroma citotoksičnosti. Rezultati preiskav in preizkusov so pokazali, da ima kompozitna membrana CipHCl-PLA/PBC/CS dobro biokompatibilnost. Pri vsebnosti CipHCl 20 w/% je povprečni premer vlaken 374 nm. Po 192 urah je bila hitrost sproščanja zdravila kompozitne membrane CipHCl-PLA/PBC/CS pri vsebnosti 20 w/% CipHCl enaka 88,2 %. Antibakterijska aktivnost izdelane vlaknaste membrane CipHCl-PLA/PBC/CS je bila precej višja od kompozitne vlaknaste membrane PLA/PBC. Poleg tega je bila antibakterijska aktivnost izdelane kompozitne vlaknaste membrane CipHCl-PLA/PBC/CS rahlo višja v prisotnosti bakterije *E. coli* kot pa pri bakteriji *S. aureus*.

Gljučne besede: polilaktatna kislina, polibutilenski karbonati, hitozan, CipHCl, antibakterijska aktivnost

1 INTRODUCTION

Electrospinning is a simple and effective manufacturing method for producing fiber structures made from a variety of biopolymers, with diameters ranging from nanometers to micrometers.^{1,2} Due to their unique properties such as tunable diameter and pore size, high porosity, high surface-to-volume ratio, morphological similarity to the extracellular matrix and surface functionality, electrospun fibers have been studied in diverse fields including drug delivery, filtration, wound dressing, tissue engineering and cell culture.³⁻⁵ In particular, the drug loading technology has attracted more and more atten-

tion from drug scientists. For example, Kataria et al.⁶ observed polyvinyl alcohol (PVA) and sodium alginate electrospun nanofibers loaded with antibiotic ciprofloxacin as transdermal patches in a wound-healing application. Results showed that the ciprofloxacin-loaded nanofibers reduced the wound healing time compared to the drug-free nanofibers.

Chitosan (CS) is a deacetylated derivative of chitin, which can be excavated in large amounts from the extraskeletal waste of crustaceans. The biodegradability, biocompatibility and non-toxic properties of CS make it a safe material for a variety of environmental and biomedical applications.^{7,8} CS has been used in various applications such as hydrogels, membranes, nanofibers, beads, micro/nanoparticles, scaffolds and sponges. Due

*Corresponding author's e-mail:
gxx218@163.com

to its biodegradability, predictable degradation rate, antibacterial activity, structural integrity, non-toxicity to cells and biocompatibility, CS allows good wound healing, tissue engineering and ophthalmic lens manufacturing.^{9,10} Because of its low solubility, low stability and low mechanical properties, electrospinning of CS is very difficult to perform. Therefore, it is necessary to mix another polymer polylactic acid (PLA) with CS to improve the mechanical properties of CS nanofibers.^{11,12} However, polylactic acid exhibits some defects in processability, such as brittleness and poor stiffness, which limit its promotion and use as a kind of electrospinning biodegradable matrix material. Polybutylene carbonate (PBC) is a new type of biodegradable polyester. PBC has excellent comprehensive properties. It is considered to be one of the most cost-effective and promising materials.^{13–15} PBC shows relatively hydrophilic properties and high tensile strength due to its chemical structure.¹⁶ In addition, as PBC is very conducive to cell attachment, its biocompatibility is similar to PLA.¹⁷ Besides, PBC can improve the hard and brittle nature of PLA, and it is well compatible with PLA. PBC can be used as a toughener to improve the brittleness of PLA.¹⁸ These co-spinning agents are a class of biodegradable polymers with good spinnability and good biocompatibility, and are conducive to an efficient application of PLA/PBC/CS composite fiber membranes.

Therefore, in this paper a CipHCl-PLA/PBC/CS composite fiber membrane was prepared using the electrostatic spinning technology. The properties of the CipHCl-PLA/PBC/CS composite fiber membrane were studied with SEM, XRD, FTIR and a drug-release test. The antibacterial properties of the composite fiber mem-

brane against *E. coli* and *S. aureus* were legally analyzed with the inhibition zone method, and the antibacterial mechanism was discussed. The composite fiber membrane has a high application value in the field of antibacterial dressings.

2 EXPERIMENTAL PART

2.1 Reagents and apparatus

Reagents: polylactic acid (PLA, $M_n = 6.08 \times 10^4$ Da) and polybutylene carbonate, (PBC, $M_n = 7.0 \times 10^5$ Da) were purchased from Hisun Biomaterials (Zhejiang Province); chitosan (CS, $M_n = 160.9$ Da, degree of deacetylation $\geq 90\%$) was purchased from Xiamen Biotechnology Co., Ltd.; ciprofloxacin hydrochloride (CipHCl) was purchased from Xiamen Yicheng Technology Co., Ltd.; trifluoroacetic acid (TFA) was purchased from Beijing Coupling Technology Co., Ltd.; the PBS phosphate buffer solution (pH = 7.2–7.4) was purchased from Tianjin Tianli Chemical Reagent Co., Ltd.; dimethyl sulfoxide (DMSC, 99.9%) was purchased from Jinan Yunxiang Chemical Co., Ltd.; peptone, beef extract and agar were purchased from Sinopharm Chemical Reagent Co., Ltd.; the MTT reagent was purchased from Biyun-tian Biotechnology Research Institute of Haimen City.

Apparatus: Fourier transform infrared spectrometer (FTIR), Spectrum One model, an American PE company; scanning electron microscope (SEM), S-4300 model, Hitachi, Japan; X-ray diffraction analyzer (XRD), D8 Advance model, Bruker-AXE, Germany; UV-visible spectrophotometer, UV-5100 B model, Shanghai Yuan Analytical Instrument Co., Ltd.; NC ultrasonic cleaner,

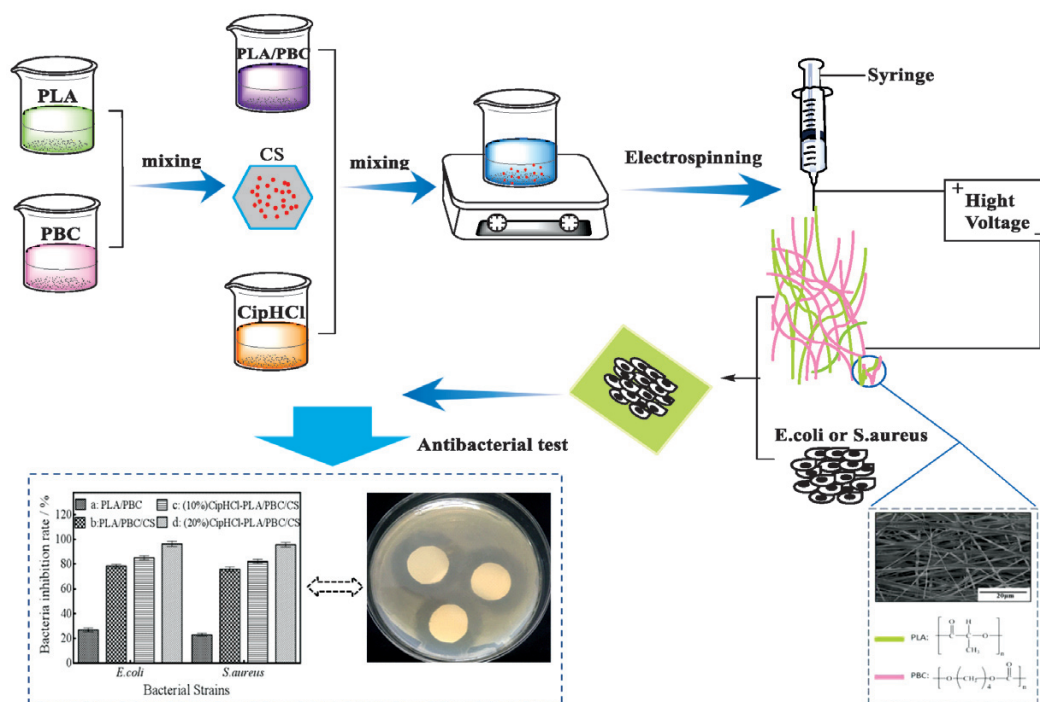


Figure 1: Schematic diagram of synthesizing the CipHCl-PLA/PBC/CS composite fiber membrane and its performance

KQ5200DE model, Kunshan Ultrasonic Instrument Co., Ltd.; heat-collecting magnetic stirrer, DF-101S model, Jintan Huafeng Instrument Co., Ltd.

2.2 Sample preparation

2.2.1 Preparation of the spinning solutions

PLA, PBC and CS were dried in a vacuum drying oven for 24 h at 37 °C. CipHCl (10 w/% and 20 w/%) was sonicated for 0.5 h at room temperature with a small amount of solvent until CipHCl was well dispersed and sealed for future use. According to the previous research of our group, 1 : 2.5 was the best mass ratio of PLA to PBC in the PLA/PBC/CS composite fiber membrane. The dried PLA, PBC and CS were dissolved in TFA to make solutions, and then the dispersed CipHCl solution in different amounts was added to the above polymer dope. Spinning solutions of CipHCl-PLA/PBC/CS were obtained.

2.2.2 Electrospinning

The polymer solution was placed in a 10 mL syringe with an inner diameter of 0.41 mm at room temperature. The syringe containing the blend solution was installed into the electrospinning machine. The height of the syringe was adjusted so that the height of the needle and the center position of the aluminum foil receiving plate were on the same horizontal line, and the distance between the needle and the receiving plate was 25 cm. The ejection speed was 0.5 mm/min. The syringe end was connected to the positive pole of the high-voltage DC power supply, and the aluminum foil receiver was connected to the negative pole. The positive voltage was 18 kV and the negative voltage was -16 kV. Polymer fibers were produced, from the tip of the needle to the grounded current collector, by the action of an external electric field. The samples were labeled as PLA/PBC, PLA/PBC/CS, 10 % CipHCl-PLA/PBC/CS and 20 % CipHCl-PLA/PBC/CS in accordance with the components. **Figure 1** shows the schematic of the formation of the CipHCl-PLA/PBC/CS composite fiber membrane.

2.3 Characterization

The chemical structures of the samples were analyzed using FTIR with an ATR accessory in a dry environment at room temperature. The scanning range was 4000–500 cm⁻¹ and the scanning resolution was less than 0.09 cm⁻¹. The morphology and microstructures of the samples were observed using SEM with an acceleration voltage of 20 kV. Prior to the analysis, the samples were coated with a thin layer of gold. A D8 Advance type X-ray diffractometer from Bruker-AXE in Germany was used for the X-ray diffraction analysis (XRD) to determine the crystal structure of the electrospun composite fiber membrane. The voltage was 50 kV, the current was 50 mA, the scanning speed was 3 °/min and the scanning range was 10°–60°.

2.4 Performance test of the composite fiber membrane

2.4.1 Drug standard curve equation

0.1 g of CipHCl was finely weighed with an electronic balance and transferred to a 100 mL volume flask. A PBS phosphate buffer solution with a pH value in the range of 7.2–7.4 was added into the flask. The solution was stirred with a glass rod, and then ultrasonic vibration was performed for 30 min. Finally, the solution was further diluted and configured as (50, 25, 12.50, 6.25, 3.125 and 1.56) µg/mL. The solutions with different concentrations were placed in cuvettes. The absorbance tests were carried out with ultraviolet spectrum at a wavelength of 270 nm to measure the absorbance of CipHCl and obtain the standard curve.

2.4.2 Determination of the drug release rate in vitro

5 mg and 10 mg of rectangular drug-loaded fiber-membrane samples were accurately weighed and placed in 100 mL volumetric flasks. To simulate in vitro drug release, the PBS buffer solution was simultaneously added to the flasks and centrifuged with a constant-temperature shaker. 5 mL of the solution was taken out after (0.5, 1, 2, 3, 4, 5, 6, 8, 12, 24, 36, 48, 60, 84, 120, 156, and 192) h and put in sample bottles. An ultraviolet spectrophotometer was used to measure the drug concentrations of the solutions at each time point. The cumulative release rate of the drug at different times was calculated as shown in Equation (1).

$$T(\%) = \frac{C_x V + V_k \sum_{k=0}^{x-k} C_k}{M_{\text{CipHCl}}} \quad (1)$$

Here, T is the cumulative release rate of the drug (%); x is the number of release media for the replacement; C_x is the sample concentration at the x -th time node, in mg/mL; V is the volume of the release medium in mL; V_k is the volume sampled at the k -th time node; C_k is the concentration of the solution sample taken at the k -th time node, in mg/mL; M_{CipHCl} is the mass of CipHCl in the composite fiber membrane containing CipHCl, in mg.

2.5 Antibacterial performance test

According to the GB/T 20944.1-2007 national standard, the in vitro antibacterial activity of two bacterial strains, *E. coli* and *S. aureus*, were evaluated with the agar-diffusion method. The composite fiber membrane was cut into a 20 mm diameter membrane and sterilized in a clean bench with ultraviolet light for 30 min prior to using. Luria broth (LB) agar plates containing 1×10^5 bacterial colony-forming units (CFU/mL) were used for culturing. After 24 h of incubation at 37 °C, the diameter of the zone of inhibition was evaluated, as shown in Equation (2).

$$Y = \frac{A-B}{A} \times 100 \% \quad (2)$$

Here, *A* is the viable count (cfu/mL) of a blank sample after 24 h of contact with the bacteria; *B* is the number of viable bacteria (cfu/mL) after 24 h of contact between the sample and the bacteria; *Y* is the antibacterial rate.

2.6 Cytotoxicity test

The extract of a sample was prepared according to the GB/T 16886.12 national standard, that is, the fiber membrane sterilized with irradiation was cut into a 10 mm circular membrane, and dimethylsulfoxide (DMSO) medium was added at a ratio of 6 cm²/mL. The extraction stock was obtained by leaching at 37 °C and a 5 % CO₂ saturated humidity. Then the extract was added to a 96-well cell culture plate, and L929 cells were inoculated with a cell density of 2.5 × 10⁴ cells/mL. MTT detection was performed after 72 h of incubation in a CO₂ incubator. After a period of time, the status of the cell growth was observed using an optical microscope. The absorbance was measured 4 times at 450 nm with a standard instrument (Bio-Rad, USA). The cell proliferation rate (*R*) was calculated with the average value of the absorbance, as shown in Equation (3).

$$R = \frac{OD_i}{OD} \times 100 \% \quad (3)$$

Here, *OD* is the absorbance value of the blank control sample, and *OD_i* is the absorbance value of the experimental group. Finally, the cytotoxicity levels were determined in accordance with the GB/T 16886.12 cytotoxicity rating standard, as shown in **Table 1**.

Table 1: Cytotoxicity rating criteria

<i>R</i> /%	≥ 100	75–99	50–74	25–49	1–24
level	0	1	2	3	4
evaluation of results	qualified	qualified	to be determined	disqualified	disqualified

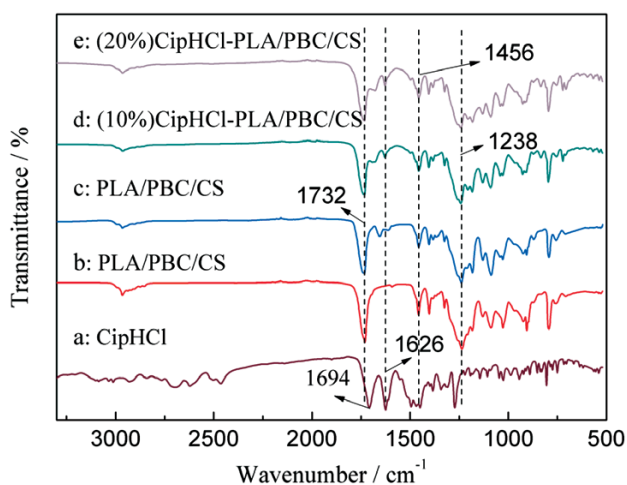


Figure 2: FTIR spectra of pure PLA/PBC sample, PLA/PBC/CS and CipHCl-PLA/PBC/CS composite fiber membranes with different CipHCl drug contents

3 RESULTS AND DISCUSSION

3.1 FTIR spectra analysis

Figure 2 illustrates the characteristic FTIR spectra of CipHCl, PLA/PBC, PLA/PBC/CS, and CipHCl-PLA/PBC/CS fiber membranes containing different amounts of CipHCl. It can be seen that the stretching vibration peak of methylene at 2966 cm⁻¹ is a structural characteristic absorption peak attributed to PBC. The stretching vibration peak of C=O at 1732 cm⁻¹ is a structural characteristic belonging to the PLA absorption peak. The adsorption peak at 1456 cm⁻¹ is ascribed to the saturated C-H bond and the adsorption peak at 1238 cm⁻¹ is ascribed to the stretching vibration of RCR=O. It can be seen from **Figure 2** that the characteristic peaks are generally consistent with the PLA/PBC sample in the PLA/PBC/CS fiber membrane, except that a characteristic peak appears at 1183 cm⁻¹. This is because -NH₂ in CS bonded with -COOH in PLA to form -NH₃⁺. When comparing the FTIR spectra of CipHCl, CipHCl-PLA/PBC/CS (10 w/%) and CipHCl-PLA/PBC/CS (20 w/%), it can be found that two more absorption peaks are apparent at 1626 cm⁻¹ and 1694 cm⁻¹, ascribed to the structural characteristic absorption peak of NH and C=O in CipHCl, respectively.

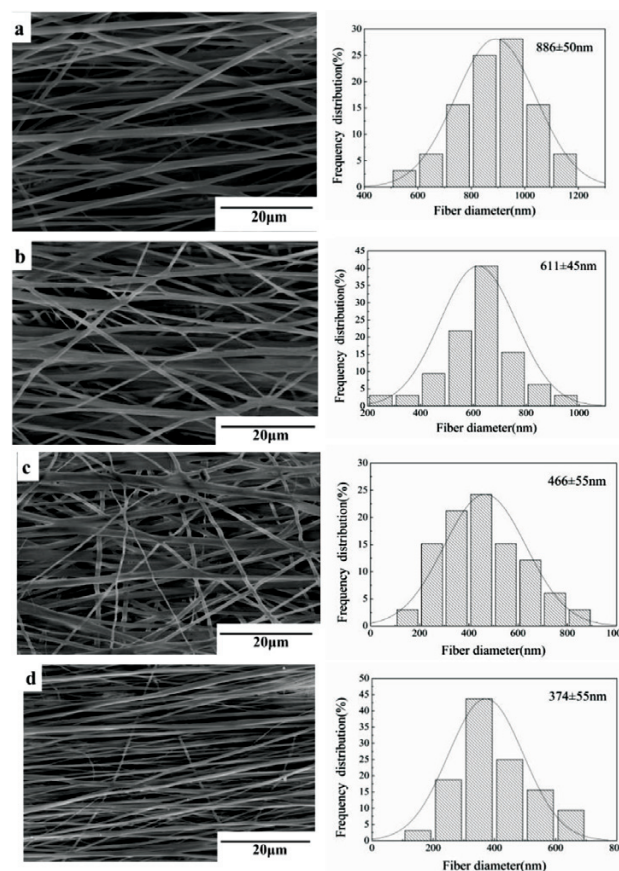


Figure 3: SEM micrographs and average diameter distributions of: a) pure PLA/PBC, b) PLA/PBC/CS, c) CipHCl-PLA/PBC/CS with 10 w/ % CipHCl, d) CipHCl-PLA/PBC/CS with 20 w/ % CipHCl

3.2 SEM image and the fiber diameter distribution analysis

Figure 3 shows the SEM images and fiber diameters of PLA/PBC, PLA/PBC/CS, CipHCl-PLA/PBC/CS (10 w%) and CipHCl-PLA/PBC/CS (20 w%) composite fiber membranes. It can be seen that the surfaces of all the fibers are relatively smooth without any bead-like structure. The average diameter of the PLA/PBC fiber in **Figure 3a** is 886 nm, and the average diameter of the PLA/PBC/CS fiber in **Figure 3b** is 611 nm, indicating that the addition of CS decreased the average diameter of the fiber membrane. When the content of CipHCl in PLA/PBC/CS is 10 w%, the average fiber diameter is 466 nm as shown in **Figure 3**. The average diameter is significantly reduced to 374 nm when the CipHCl content is 20 w%. Besides, the content of drug CipHCl has a significant effect on the fiber diameter. As shown in **Figure 3d**, the fiber diameter decreases and its distribution becomes more uniform with the increase in the CipHCl content. This is because CipHCl contains more polar groups (hydroxyl groups), which increase the conductivity of the polymer dope and lead to a greater degree of refinement of the jet stream during the electrospinning process.¹⁹ It is more conducive to the loading and release of drug molecules because the gap between the fibers becomes larger. Therefore, it has great potential to be used as a good medical carrier material.

3.3 X-ray diffraction patterns

As shown in **Figure 4**, the XRD patterns of CipHCl, PLA/PBC, PLA/PBC/CS, CipHCl-PLA/PBC/CS (10 w%) and CipHCl-PLA/PBC/CS (20 w%) composite fiber membranes explain the crystalline structure and distribution of small drug molecules in the fibrous membrane. The PLA/PBC fiber membranes have characteristic diffraction peaks at 21.71° and 22.95°, belonging to

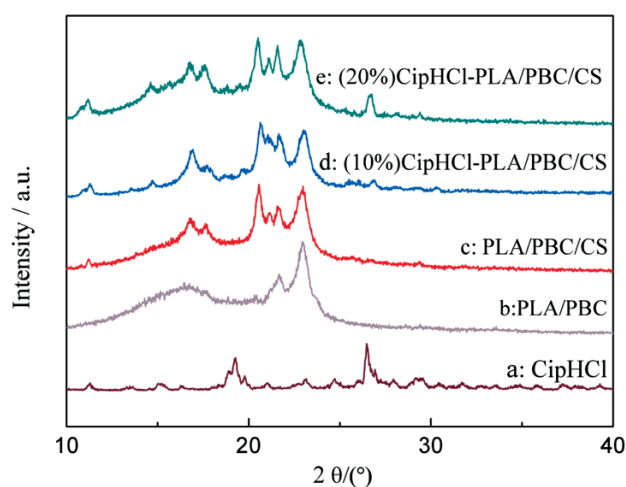


Figure 4: XRD patterns of CipHCl powder, pure PLA/PBC composite fiber membrane, PLA/PBC/CS composite fiber membrane and CipHCl-PLA/PBC/CS composite fiber membrane with different drug contents

PBC and PLA, respectively. Upon the addition of CS, two new 2θ peaks appeared at 16.82° and 20.42°, and the characteristic diffraction peaks remain unchanged for PLA/PBC, indicating that the crystal structure did not change and there is no interaction between CS and PLA/PBC. The CipHCl crystal shows the characteristic diffraction peaks at 2θ of 11.18°, 19.22°, 23.05°, 24.77° and 26.48°. The characteristic diffraction peaks appear at 11.18° and 26.48° on each drug-loaded fiber membrane. It can be seen that the higher the content of ciprofloxacin hydrochloride, the more pronounced is the peak shape. It can be seen that the addition of CipHCl did not change the crystalline structure of the PLA/PBC/CS fiber membrane, indicating that the small drug molecules are uniformly distributed in the crystalline phase of the polymer.

3.4 In vitro drug release analysis

Figure 5 shows the UV spectra of CipHCl solutions in the phosphate buffer at different concentrations of (50, 25, 12.50, 6.25, 3.125 and 1.56) $\mu\text{g/mL}$. **Table 2** lists the absorbance of CipHCl at different concentrations. **Figure 6** shows the standard curve. The concentration of CipHCl is linearly proportional to the absorbance.

Table 2: Absorbance intensity of CipHCl at different concentrations

Concentration ($\mu\text{g/mL}$)	Wavelength (nm)	Absorbance
1.560	270.87	0.15
3.125	270.76	0.25
6.250	270.58	0.37
12.50	270.02	0.48
25.00	270.09	0.59
50.00	270.02	0.72

The plots from **Figure 6** were fitted to the linear Equation (4) based on the regression curve.

$$Y = 0.0563 X + 0.0372 \quad R_2 = 0.9994 \quad (4)$$

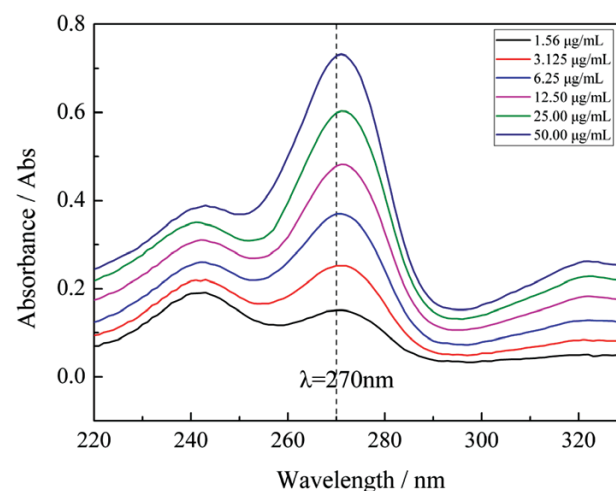


Figure 5: UV spectra of CipHCl aqueous solutions with various CipHCl concentrations of (50, 25, 12.50, 6.25, 3.125 and 1.56) $\mu\text{g/mL}$

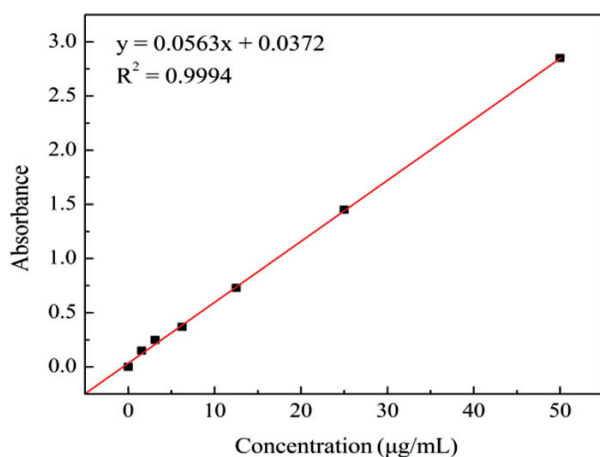


Figure 6: Standard curve between the UV absorbance intensity and the concentration of CipHCl in phosphate buffer (pH = 7.4)

Here, Y is the absorbance intensity in the UV spectrum, and X ($\mu\text{g/mL}$) is the concentration of CipHCl. As shown in **Figure 5**, the plots are in good agreement with the fitted curve, indicating a linear relationship between the concentration of CipHCl and the absorbance intensity. Thus, the fitted formula was employed as the standard curve for drug release in vitro.

Figure 7 shows the release-rate curves for the CipHCl in the CipHCl-PLA/PBC/CS composite fiber membrane with CipHCl contents of 10 w/% and 20 w/%. It can be seen that the release rates of the fiber membranes increase with the increase in the drug content. The rate curves in **Figure 7** can be divided into three stages. In the initial drug-release stage (from 0–8 h), the drug-release rate was low. The released amount reached 12.5 % and 25.1 % after 8 h for the samples with CipHCl contents of 10 w/% and 20 w/%, respectively. Subsequently, the released-drug amount raised slowly after 84 h. The released amount reached 66.5 % and 77.2 % for the samples with CipHCl contents of 10 w/% and 20 w/%, respectively, after 84 h. Finally, the release rate

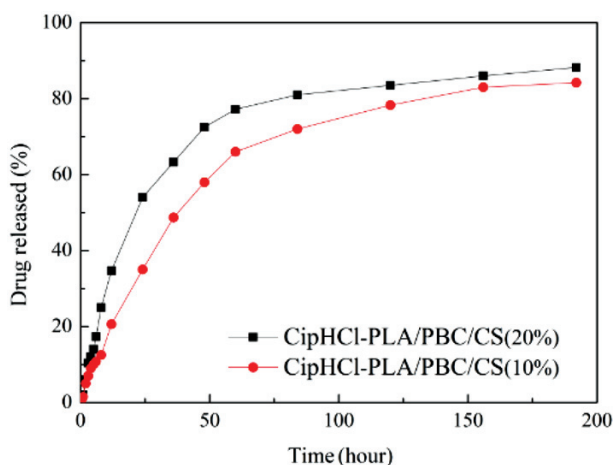


Figure 7: In vitro drug release profiles of CipHCl-PLA/PBC/CS composite fiber membranes with different CipHCl contents

turned very slow and the drug-release amount reached the limits of 84.2 % and 88.3 % for the samples with CipHCl contents of 10 w/% and 20 w/%, respectively, after 192 h. According to **Table 2**, the release rate of the membrane sample with a high CipHCl drug content was higher than that of the sample with a low CipHCl content. In the drug-release system, a high release rate can allow a larger drug amount to reach the target site in a shorter time, achieving the antibacterial effect. So the sample with the 20 w/% CipHCl content is better than the sample with the 10 w/% CipHCl content.

3.5 Antibacterial performance analysis

Figures 8a, 8b, 8c and **8d** show the pictures of different composite membranes cultured with *E. coli*. **Figures 8e, 8f, 8g** and **8h** show the pictures of different membranes cultured with *S. aureus*. The antibacterial width of each sample is shown in **Figure 9**. As shown in **Figures 8a** and **8e**, there was no bacteriostatic zone around the PLA/PBC fiber membrane, which indicates that the

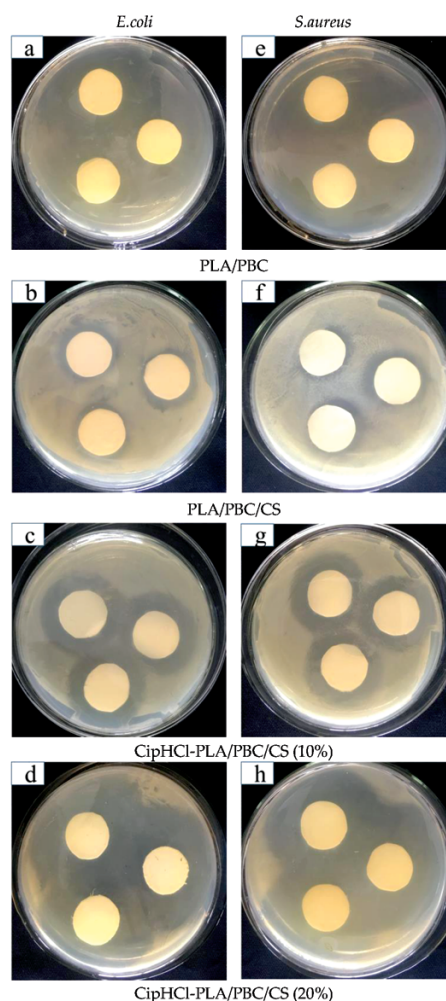


Figure 8: Pictures of different membranes cultured with *E. coli* and *S. aureus*

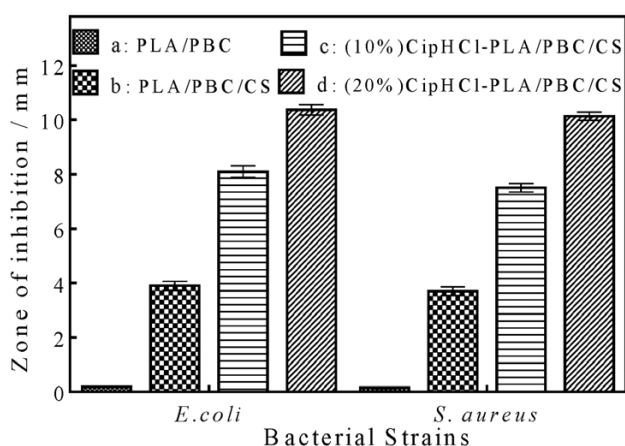


Figure 9: Antibacterial zone width of PLA/PBC, PLA/PBC/CS and CipHCl-PLA/PBC/CS composite fiber membranes with different drug contents

PLA/PBC fiber membrane has almost no antibacterial effect on *E. coli* and *S. aureus*. When CS is added (as shown in **Figures 8b** and **8f**), the width of the inhibition zone around the sample increases and the width of the inhibition zone for *E. coli* and *S. aureus* is 3.9 mm and 3.7 mm, respectively. Due to its large width of the bacteria inhibition zone, it can be concluded that the PLA/PBC/CS membrane is a material with a good antibacterial effect according to the Chinese national standard.

As shown in **Figures 8c** and **8g**, the width of the inhibition zone for *E. coli* and *S. aureus* increases to 8.1 mm and 7.5 mm, respectively, for CipHCl-PLA/PBC/CS with 10 w/% of CipHCl. The width of the inhibition zone for *E. coli* and *S. aureus* further increases to 10.5 mm and 10.1 mm, respectively, when the content of CipHCl is 20 w/%. (as shown in **Figures 8d** and **8h**). The CipHCl-PLA/PBC/CS membranes can be defined as a material with an excellent antibacterial effect. The addition of CipHCl significantly improves the antibacterial performance of the composite fiber membranes. The higher the CipHCl amount, the better is the antibacterial effect. The reason is that the CS macromolecules were adsorbed on the surface of the bacteria to form a polymer film, hindering the transport of nutrients into the cells and thus inhibiting the bacteria. The introduction of CipHCl can destroy the morphological structures of the bacteria. This leads to the bacterial death and achieves bacteriostatic effects.^{20,21} In addition, it can be concluded that the composite fiber membrane has a better antibacterial effect on *E. coli* than *S. aureus*.

Figure 10 shows the inhibition rates of four composite fiber membranes (PLA/PBC, PLA/PBC/CS, CipHCl-PLA/PBC/CS (10 w/%) and CipHCl-PLA/PBC/CS (20 w/%) for *E. coli* and *S. aureus* detected with the colony-recovery method. It can be seen that the antibacterial rates of the four composite fiber membranes for *E. coli* were (26.8, 78.4, 85.2 and 96.4) %, and the antibacterial rates for *S. aureus* were (22.9, 76.7, 82.3 and 95.8) %, respectively. These results indicate that the antibacterial

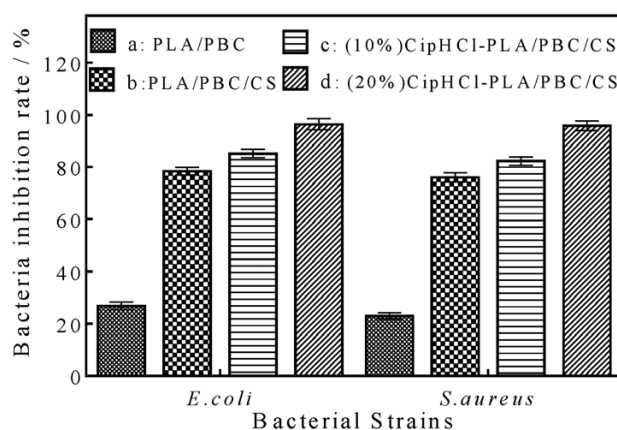


Figure 10: Bacteriostatic rate of PLA/PBC, PLA/PBC/CS and CipHCl-PLA/PBC/CS composite fiber membranes with different drug contents

activity of the PLA/PBC composite fiber membrane was not obvious and the antibacterial rate was significantly improved after adding CS and CipHCl. The antibacterial effect was better with the increase in the CipHCl drug content. The antibacterial rate of each fiber membrane sample for *E. coli* was slightly higher than that for *S. aureus*. The result is consistent with the antibacterial circle experiment.

3.6 Cytotoxicity test

In order to study the cellular compatibility of the PLA/PBC/CS and CipHCl-PLA/PBC/CS composite fiber membranes, an inverted microscope was used to observe the morphology of the L929 cells on the obtained ultrathin electrospinning film after durations of (1, 3 and 7) d. The results are shown in **Figures 11b**, **11d** and **11f**, representing the cell morphologies on the CipHCl-PLA/PBC/CS composite fiber membranes, while **Figures 11a**, **11c** and **11e** represent the cell morphologies on the PLA/PBC/CS composite fiber membranes, being the control samples. The cells in the photo are spindly and of a uniform size. They have smooth cell walls,

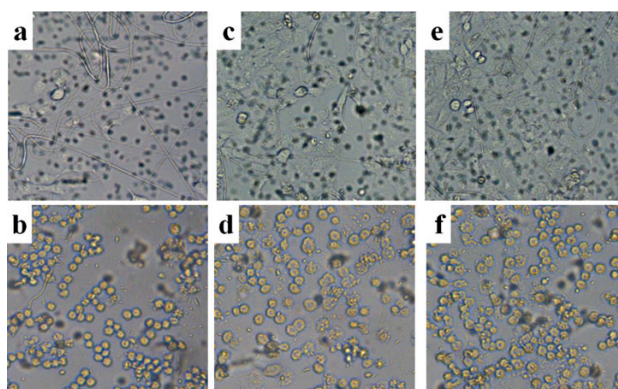


Figure 11: Inverted microscopy images of L929 cells grown on PLA/PBC/CS (a, c, e) and CipHCl-PLA/PBC/CS (b, d, f) composite fiber membranes after 1 d (a, b), 3 d (c, d), and 7 d (e, f)

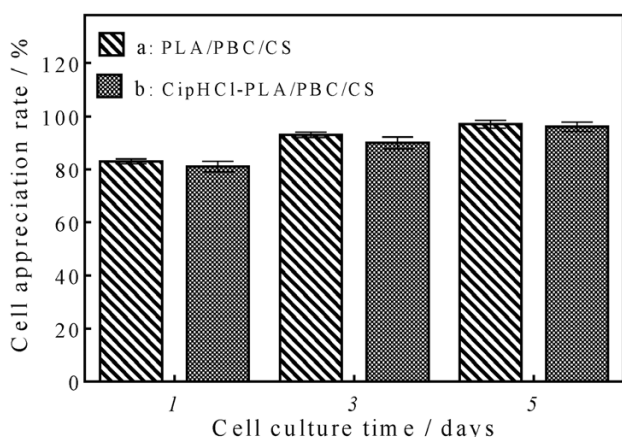


Figure 12: In vitro cytotoxicity of PLA/PBC/CS and CipHCl-PLA/PBC/CS composite fiber membranes to L929 cells

growing well. Hence, the composite fiber membrane shows good cellular compatibility and can be used for drug-release applications.

As an effective drug carrier, a fiber membrane must be nontoxic and antibacterial. Herein, to explore the cytotoxicity of the prepared fiber membranes, an MTT assay was employed with the L929 cells to detect membrane toxicity. The results are shown in **Figure 12**. The CipHCl-PLA/PBC/CS and PLA/PBC/CS composite membranes showed low cytotoxicity to the L929 cells, and the cellular growth rate was not less than 80 % after (1, 3 and 7) d. According to the GB/T 16886.12, the toxicity of both tested membranes to cells met the standard of grade 1. The fiber membranes were non-toxic and met the standards of implantable medical materials. Therefore, it can be concluded that the prepared CipHCl-PLA/PBC/CS composite fiber membrane is non-toxic.

4 CONCLUSIONS

A ciprofloxacin hydrochloride (CipHCl)-polylactic acid (PLA)/polybutylene carbonate (PBC)/chitosan (CS) new component composite fiber membrane was successfully prepared with the electrostatic spinning technology. The fiber diameter decreased upon the addition of CS and CipHCl. The drug-release test results for the drug-loaded composite fiber membrane showed that the drug-release rate changed. When the content of CipHCl was 20 w/%, the antibacterial widths of *E. coli* and *S. aureus* were 10.5 mm and 10.1 mm, and the antibacterial rates were 96.4 % and 95.8 %, respectively. According to the results of the material's toxicity test and analysis, the prepared CipHCl-PLA/PBC/CS composite fiber membrane is non-toxic and meets the standards for implantable medical materials. It can be concluded that the CipHCl-PLA/PBC/CS composite fiber membrane can be used as a good medical carrier material because of its excellent antibacterial property and excellent drug-release ability. So, it has a great application potential for wound dressings.

Acknowledgment

The authors gratefully acknowledge the support from the Heilongjiang Provincial Department of Education Project (CLKFKT2021Z3, 145109301), China.

5 REFERENCES

- Z. Saadi, A. Rasmont, G. Cesar, H. Bewa, L. Benguigui, Fungal degradation of poly(L-lactide) in soil and in compost, *Journal of Polymers and the Environment*, 20 (2012), 273–282, doi:10.1007/s10924-011-0399-9
- M. M. Cui, L. L. Liu, N. Guo, R. X. Su, F. Ma, Preparation, Cell Compatibility and Degradability of Collagen-Modified Poly(lactic acid), *Molecules*, 20 (2015) 1, 595–607, doi:10.3390/molecules20010595
- J. Fal, K. Bulanda, J. Traciak, J. Sobczak, R. Kuziola, K. Maria, G. Budzik, M. Oleksy, G. Żyła, Electrical and Optical Properties of Silicon Oxide Lignin Polylactide (SiO₂-L-PLA), *Molecules*, 25 (2020) 6, 1354, doi:10.3390/molecules25061354
- Z. Y. Tang, F. L. Fan, Z. Z. Chu, C. L. Fan, Y. Y. Qin, Barrier properties and characterizations of poly(lactic acid)/ZnO nanocomposites, *Molecules*, 25 (2020) 6, 1310, doi:10.3390/molecules25061310
- J. Zeng, L. Yang, Q. Liang, Influence of the drug compatibility with polymer solution on the release kinetics of electrospun fiber formulation, *J. Controlled Release*, 105 (2005) 1/2, 43–51, doi:10.1016/j.jconrel.2005.02.024
- R. Y. Yang, D. Y. Wang, H. L. Li, Y. He, X. Y. Zheng, M. W. Yuan, M. L. Yuan, Preparation and characterization of bletilla striata polysaccharide/polylactic acid composite, *Molecules*, 24 (2019) 11, 2104, doi:10.3390/molecules24112104
- I. Cerkez, A. Sezer, S. K. Bhullar, Fabrication and characterization of electrospun poly(ϵ -caprolactone) fibrous membrane with antibacterial functionality, *R. Soc. Open Sci.*, 4 (2017) 2, 160911, doi:10.1098/rsos.160911
- K. Vidyakshmi, K. N. Rashmi, T. M. P. K. Siddaramaiah, Studies on formulation and in vitro evaluation of pva/chitosan blend films for drug delivery, *J. Macromol. Sci. A*, 41 (2004), 1115–1122, doi:10.1081/MA-200026554
- H. Chi, W. H. Li, C. L. Fan, C. Zhang, L. Li, Y. Y. Qin, M. L. Yuan, Effect of high pressure treatment on poly(lactic acid)/nano-TiO₂ composite films, *Molecules*, 23 (2018) 10, 2621, doi:10.3390/molecules23102621
- J. K. Xu, S. Strandman, J. L. X. Zhu, J. Barralet, M. Cerruti, Genipin-crosslinked catechol-chitosan mucoadhesive hydrogels for buccal drug delivery, *Biomaterials*, 37 (2015), 395, doi:10.1016/j.biomaterials.2014.10.024
- P. Taepaiboon, U. Rdthongungsar, P. Supaphol, Drug-loaded electrospun mats of poly(vinyl alcohol) fibres and their release characteristics of four model drugs, *Nanotechnology*, 17 (2006) 9, 2317–2329, doi:10.1088/0957-4484/17/9/041
- M. S. Austero, A. E. Donius, U. G. K. Wegst, C. L. Schauer, New crosslinkers for electrospun chitosan fibre mats, *J. R. Soc. Interface*, 9 (2012), 2551–2562, doi:10.1098/rsif.2012.0241
- E. Fortunati, F. Luzi, D. Puglia, R. Petrucci, J. M. Kenny, L. Torre, Processing of PLA nanocomposites with cellulose nanocrystals extracted from *Posidonia oceanica* waste: Innovative reuse of coastal plant, *Ind. Crops Prod.*, 67 (2015), 439–447, doi:10.1016/j.indcrop.2015.01.075
- A. J. R. Lasprilla, G. A. R. Martinez, B. H. Lunelli, A. L. Jardini, R. Maciel Filho, Poly-lactic acid synthesis for application in biomedical devices – A review, *Biotechnol. Adv.*, 30 (2012) 1, 321–328, doi:10.1016/j.biotechadv.2011.06.019
- G. Giammona, E. F. Craparo, Biomedical applications of polylactide (PLA) and its copolymers, *Molecules*, 23 (2018) 4, 980, doi:10.3390/molecules23040980

- ¹⁶ D. Q. Liu, Z. Q. Cheng, et al., Polycaprolactone nanofibres loaded with 20(S)-protopanaxadiol for in vitro and in vivo anti-tumour activity study, *R. Soc. Open Science*, **5** (2018), doi:10.1098/rsos.180137
- ¹⁷ K. Mäenpää, V. Ellä, J. Mauno, M. Kellomäki, R. Suuronen, T. Ylikomi, S. Miettinen, Use of adipose stem cells and polylactide discs for tissue engineering of the temporomandibular joint disc, *J. R. Soc., Interface*, **7** (2010), 177–188, doi:10.1098/rsif.2009.0117
- ¹⁸ R. Sakai, B. John, M. Okamoto, J. V. Seppälä, J. Vaithilingam, H. Hussein, Fabrication of polylactide-based biodegradable thermoset scaffolds for tissue engineering applications, *Macromol. Mater. Eng.*, **298** (2013), 45–52, doi:10.1002/mame.201100436
- ¹⁹ J. Jeong, M. Ayyoob, J. H. Kim, In situ formation of PLA-grafted alkoxysilanes for toughening a biodegradable PLA stereocomplex thin film, *RSC Adv.*, **9** (2019) 38, 21748–21759, doi:10.1039/C9RA03299A
- ²⁰ Y. B. Zhu, Y. Wang, J. Y. Z. Xu, J. H. Chen, L. M. Wang, B. Qi, Enantioselective biosynthesis of l-phenyllactic acid by whole cells of recombinant *Escherichia coli*, *Molecules*, **22** (2017) 11, 1966, doi:10.3390/molecules22111966
- ²¹ W. Shao, S. X. Wang, X. F. Liu, Tetracycline hydrochloride loaded regenerated cellulose composite membranes with controlled release and efficient antibacterial performance, *RSC Adv.*, **6** (2016) 4, 3068–3073, doi:10.1039/C5RA23409C